

CONFORMERS OF *TRANS-N*-METHYLACETAMIDE Ab initio study of geometries and vibrational spectra*

NOEMI G. MIRKIN and SAMUEL KRIMM

Biophysics Research Division and Department of Physics, University of Michigan, Ann Arbor,
MI 48109 (U.S.A.)

(Received 15 June 1990)

ABSTRACT

Energies and geometries have been obtained, at the 4-31G* level, for the four stable conformers of *trans-N*-methylacetamide that result from conformational isomerism of the CH₃ groups. Ab initio force fields were obtained for these four structures, and the force constants were scaled to experimental matrix-isolated frequencies. The results show that the conformers should be spectroscopically distinguishable, and in fact the observed bands can be satisfactorily assigned on this basis without invoking a non-planar amide group. Conformational isomerism may also be partly responsible for the unusual breadth of the amide V band.

INTRODUCTION

N-Methylacetamide (NMA) has been the subject of extensive spectroscopic study, both experimental [1–18] and theoretical [6–8,14,19–25], since it is the simplest model molecule for the peptide group in proteins. It is usually found in the *trans* form (*t*-NMA), since the *cis* form (*c*-NMA) is of intrinsically higher energy, estimated to be 2.3–2.6 kcal mol^{−1} [14,26,27]. However, the *cis* form has been observed in aqueous solution by NMR [26,28] and *cis* amide groups were found in some proteins by X-ray crystallography [29].

In the process of determining the vibrational dynamics of *c*-NMA by ab initio methods [30], we have been led to re-examine the studies on *t*-NMA. It became clear that insufficient attention had been given to the spectroscopic consequences of conformational isomerism in this molecule. As we will show below, the various conformers of *t*-NMA have energies within a few tenths of a kcal mol^{−1} of each other. Thus, if this molecule is frozen in an inert gas matrix [9–11,14], we should expect to see evidence for the various conformers if they are spectroscopically distinguishable, particularly if deposition takes place from nozzles at different temperatures [14]. This possibility has not

*Dedicated to Professor Masamichi Tsuboi on the occasion of his 65th birthday.

been considered in previous analyses of the matrix spectra [9–11,14,24]; in fact, it has been assumed that different torsional states of the CH₃ groups are not likely to lead to frequency differences of the kind observed [9]. We will show that such conformers are indeed distinguishable, and that the predicted results permit an understanding of hitherto unaccounted for details in the spectra.

We studied this problem by calculating ab initio force fields for the stable conformers of *t*-NMA. The force constants were all scaled identically, based on assignments of observed matrix-isolated frequencies to the calculated modes of the lowest energy structure. A comparison of predicted frequencies of the four stable structures with observed spectra [9,10,14] shows that almost all details in these spectra can be accounted for on the basis of the presence of different conformers of *t*-NMA. This may obviate the need to explain these observations in terms of a non-planar amide group [10,11].

TABLE 1

Relative ab initio energies (in kcal mol⁻¹) of equilibrium conformers of *trans*-*N*-methylacetamide

Conformer	3-21G** ^a	4-31G	4-31G*	6-31G	6-31G*
I	0	0.06	0.07	0.10	0.21
II	0.27	0	0	0.01	0.08
III	0.57	0.17	0.09	0.11	0.14
IV	1.31	0.10	0.01	0	0

^a3-21G and 3-21G* give the same relative energies.

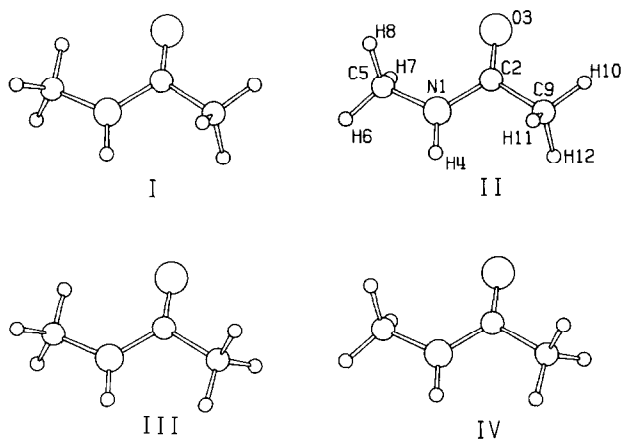


Fig. 1. Equilibrium conformers of *trans*-*N*-methylacetamide.

TABLE 2

Optimized 4-31G* geometric parameters of conformers of *trans*-*N*-methylacetamide

Parameter ^a	Conformer				Experimental ^b
	I	II	III	IV	
CC	1.514	1.514	1.514	1.513	1.520
CO	1.197	1.197	1.198	1.199	1.224
CN	1.353	1.351	1.350	1.348	1.386
NH	0.994	0.992	0.993	0.992	
NC	1.443	1.444	1.443	1.444	1.468
(N)CH ^c	1.077	1.081	1.077	1.081	1.106
(N)CH ^d	1.084	1.082	1.084	1.082	1.106
(C)CH ^c	1.079	1.079	1.083	1.083	1.106
(C)CH ^d	1.085	1.085	1.083	1.083	1.106
CCN	114.4	115.1	115.6	116.2	114.1
OCN	1023.3	122.2	123.4	122.3	121.8
CNH	118.5	119.5	118.7	119.7	110.0
CNC	123.5	121.4	123.1	121.3	119.6
NCH ^c	108.1	108.7	108.2	108.7	
NCH ^d	111.1	111.0	111.0	110.9	
CCH ^c	108.8	108.9	113.9	113.7	
CCH ^d	110.7	110.7	108.5	108.5	
OCNH	180.0	180.0	180.0	180.0	
OCNC	0.0	0.0	0.0	0.0	
CCNH	0.0	0.0	0.0	0.0	
CNCH ^c	0.0	180.0	0.0	180.0	
CNCH ^d	-119.5	60.2	-119.5	60.2	
CNCH ^d	119.5	-60.2	119.5	-60.2	
NCCH ^c	180.0	180.0	0.0	0.0	
NCCH ^d	-59.8	-59.8	-121.7	-121.7	
NCCH ^d	59.8	59.8	121.7	121.7	

^aBond lengths in Å, bond angles in degrees. ^bFrom [31]. ^cIn-plane H atom. ^dOut-of-plane H atoms.

ENERGIES AND GEOMETRIES

The *ab initio* Hartree-Fock calculations were done using Gaussian 86. We determined the equilibrium geometry of each conformer from a minimization of the total energy using the gradient method and with simultaneous relaxation of all geometric parameters and no initial assumption of planar symmetry. These calculations were carried out at the 3-21G, 3-21G*, 4-31G, 4-31G*, 6-31G, and 6-31G* levels.

The relative energies of the four conformers for which equilibrium geometries were found with these basis sets are given in Table 1. The conformer structures are shown in Fig. 1, and can be characterized by the *cis* or *trans*

TABLE 3

Internal coordinates of *trans*-*N*-methylacetamide^a

$R_1 = \Delta r(C_2-N_1)$	$R_{18} = \Delta\theta(C_2-C_9-H_{10})$
$R_2 = \Delta r(C_2-O_3)$	$R_{19} = \Delta\theta(C_2-C_9-H_{11})$
$R_3 = \Delta r(C_2-C_9)$	$R_{20} = \Delta\theta(C_2-C_9-H_{12})$
$R_4 = \Delta r(N_1-C_5)$	$R_{21} = \Delta\theta(H_{10}-C_9-H_{11})$
$R_5 = \Delta r(N_1-H_4)$	$R_{22} = \Delta\theta(H_{10}-C_9-H_{12})$
$R_6 = \Delta r(C_9-H_{10})$	$R_{23} = \Delta\theta(H_{11}-C_9-H_{12})$
$R_7 = \Delta r(C_9-H_{11})$	$R_{24} = \Delta\theta(N_1-C_5-H_6)$
$R_8 = \Delta r(C_9-H_{12})$	$R_{25} = \Delta\theta(N_1-C_5-H_7)$
$R_9 = \Delta r(C_5-H_6)$	$R_{26} = \Delta\theta(N_1-C_5-H_8)$
$R_{10} = \Delta r(C_5-H_7)$	$R_{27} = \Delta\theta(H_6-C_5-H_7)$
$R_{11} = \Delta r(C_5-H_8)$	$R_{28} = \Delta\theta(H_6-C_5-H_8)$
$R_{12} = \Delta\theta(C_9-C_2-O_3)$	$R_{29} = \Delta\theta(H_7-C_5-H_8)$
$R_{13} = \Delta\theta(C_9-C_2-N_1)$	$R_{30} = \Delta\omega(C_2O_3)$
$R_{14} = \Delta\theta(O_3-C_2-N_1)$	$R_{31} = \Delta\omega(N_1H_4)$
$R_{15} = \Delta\theta(C_2-N_1-C_5)$	$R_{32} = \Delta\tau(C_2N_1)$
$R_{16} = \Delta\theta(C_2-N_1-H_4)$	$R_{33} = \Delta\tau(C_9C_2)$
$R_{17} = \Delta\theta(C_5-N_1-H_4)$	$R_{34} = \Delta\tau(N_1C_5)$

^aFor atom numbering see Fig. 1.

relationship of an adjoining CH₃ group H atom to (C)O and (N)H: I-*cis-trans*, II-*cis-cis*, III-*trans-trans*, IV-*trans-cis*. The order of stability differs with the basis set, although for 4-31G* and 6-31G* the structures II and IV are the lowest compared to I and III. For these basis sets we see that in any case the energy differences are expected to be quite small, making it very likely that all four conformers would be present, albeit in different proportions, in the vapor at room temperature.

Normal mode calculations showed essentially no differences between 4-31G* and 6-31G* frequencies, and we therefore used 4-31G* in subsequent calculations. The equilibrium structures of the four conformers with this basis set are shown in Table 2. Also shown are some experimental values of parameters obtained from electron diffraction studies [31]. As expected [32], there is a discrepancy between observed and calculated values. We used the ab initio geometry to obtain the force constants since we wished to examine the effects on the frequencies of geometric changes between conformers. These differences, though seemingly small (up to 0.003 Å in some bond lengths and ~3° in some bond angles), can have a significant effect on vibrational frequencies.

FORCE CONSTANTS AND VIBRATIONAL FREQUENCIES

Force constants were calculated by computing analytically the second derivative of the energy at the Hartree-Fock level for the optimized 4-31G* geometries of each of the four conformers. Since the normal mode calculations were

TABLE 4

Symmetry coordinates of *trans*-*N*-methylacetamide^a

Symmetry coordinate	Description ^b
A' Modes	
$S_1 = R_1$	CN s
$S_2 = R_2$	CO s
$S_3 = R_3$	CC s
$S_4 = R_4$	NC s
$S_5 = R_5$	NH s
$S_6 = R_6 + R_7 + R_8$	CCH ₃ ss
$S_7 = 2R_6 - R_7 - R_8$	CCH ₃ as
$S_8 = R_9 + R_{10} + R_{11}$	NCH ₃ ss
$S_9 = 2R_9 - R_{10} - R_{11}$	NCH ₃ as
$S_{10} = 2R_{13} - R_{12} - R_{14}$	CCN d
$S_{11} = R_{12} - R_{14}$	CO ib
$S_{12} = R_{12} + R_{13} + R_{14}$	Red 1
$S_{13} = 2R_{15} - R_{16} - R_{17}$	CNC d
$S_{14} = R_{16} - R_{17}$	NH ib
$S_{15} = R_{15} + R_{16} + R_{17}$	Red 2
$S_{16} = R_{21} + R_{22} + R_{23} - R_{18} - R_{19} - R_{20}$	CCH ₃ sb
$S_{17} = 2R_{18} - R_{19} - R_{20}$	CCH ₃ r
$S_{18} = 2R_{23} - R_{21} - R_{22}$	CCH ₃ ab
$S_{19} = R_{18} + R_{19} + R_{20} + R_{21} + R_{22} + R_{23}$	Red 3
$S_{20} = R_{27} + R_{28} + R_{29} - R_{24} - R_{25} - R_{26}$	NCH ₃ sb
$S_{21} = 2R_{24} - R_{25} - R_{26}$	NCH ₃ r
$S_{22} = 2R_{29} - R_{27} - R_{28}$	NCH ₃ ab
$S_{23} = R_{24} + R_{25} + R_{26} + R_{27} + R_{28} + R_{29}$	Red 4
A'' Modes	
$S_{24} = R_7 - R_8$	CCH ₃ as
$S_{25} = R_{10} - R_{11}$	NCH ₃ as
$S_{26} = R_{19} - R_{20}$	CCH ₃ r
$S_{27} = R_{22} - R_{21}$	CCH ₃ ab
$S_{28} = R_{25} - R_{26}$	NCH ₃ r
$S_{29} = R_{28} - R_{27}$	NCH ₃ ab
$S_{30} = R_{30}$	CO ob
$S_{31} = R_{31}$	NH ob
$S_{32} = R_{32}$	CN t
$S_{33} = R_{33}$	CC t
$S_{34} = R_{34}$	NC t

^aCoordinates given for conformer II. Normalization constants are not shown.^bs=stretch, ss=symmetric stretch, as=antisymmetric stretch, sb=symmetric bend, ab=antisymmetric bend, ib=in-plane bend, ob=out-of-plane bend, d=deformation, r=rock, t=torsion, Red=redundancy.

TABLE 5

Scale factors for *trans*-*N*-methylacetamide

Internal coordinate	Scale factor
CN stretch	0.740
CO stretch	0.717
CC stretch and NC stretch	0.859
NH stretch	0.808
CH stretch	0.826
Non-hydrogen in-plane deformations	0.998
CNH bend	0.763
NCH bend and CCH bend	0.782
HCH bend	0.778
Out-of-plane bend and torsion	0.880

done using the Wilson GF method [33], we transformed these force constants in cartesian coordinates to force constants in internal coordinates. The internal coordinates for *t*-NMA are given in Table 3, and Table 4 gives the set of local symmetry coordinates (shown for conformer II) used in the normal mode calculations, reflecting the plane of symmetry obtained for the equilibrium structure. Of the 30 normal modes of vibration, 19 are in-plane (A') and 11 are out-of-plane (A'').

As is well known [32], frequencies calculated with *ab initio* force constants are 10–30% higher than experimental frequencies, primarily due to limitations in the basis set and neglect of electron correlation. In order to obtain a realistic representation of spectral changes due to differences in conformation, we therefore decided to scale the force constants to reproduce the observed frequencies. Separate scale factors were defined for the different types of internal coordinates and then determined by a least squares fitting of the calculated to the observed frequencies (all of the latter being assigned the same weight). In this procedure, the off-diagonal force constants F_{ij} were scaled according to $(c_i c_j)^{1/2}$, where c_i and c_j are the scale factors for F_{ii} and F_{jj} , respectively [32].

Since the *ab initio* calculation refers to an isolated molecule, it would be most appropriate to scale the calculated frequencies to the experimental gas phase frequencies [3,24]. However, these data are not of high enough quality at the present time to permit distinguishing between different conformers. The N_2 and Ar matrix-isolated spectra [9,10,14] do contain this level of detail, and we have therefore used them in the refinement process. Although these frequencies are shifted slightly compared to the gas phase, probably indicating some interaction between the NMA and the matrix, they are close enough to serve as essentially isolated-molecule (certainly not hydrogen-bonded) modes. Conformer II is of lowest energy in 4-31G*, with conformer IV being very close and generally giving similar frequencies (in 6-31G* the order in energy is reversed,

TABLE 6

Scaled diagonal force constants of *trans*-*N*-methylacetamide

Force constant ^a	Value ^b			
	I	II	III	IV
A' Modes				
CN s	5.945	5.966	6.034	6.051
CO s	10.939	10.984	10.844	10.895
CC s	4.275	4.279	4.290	4.294
NC s	5.365	5.388	5.356	5.385
NH s	6.722	6.775	6.772	6.821
CCH ₃ ss	4.950	4.949	4.954	4.955
CCH ₃ as	4.911	4.908	4.821	4.820
NCH ₃ ss	4.978	4.979	4.981	4.982
NCH ₃ as	4.951	4.847	4.955	4.849
CCN d	1.295	1.246	1.346	1.290
CO ib	1.474	1.412	1.448	1.384
CNC d	0.956	0.846	0.971	0.857
NH ib	0.503	0.501	0.506	0.503
CCH ₃ sb	0.530	0.530	0.538	0.537
CCH ₃ r	0.602	0.600	0.607	0.604
CCH ₃ ab	0.521	0.521	0.516	0.516
NCH ₃ sb	0.601	0.606	0.601	0.607
NCH ₃ r	0.757	0.761	0.756	0.761
NCH ₃ ab	0.546	0.543	0.544	0.541
A'' Modes				
CCH ₃ as	4.756	4.755	4.848	4.848
NCH ₃ as	4.699	4.798	4.704	4.804
CCH ₃ r	0.544	0.543	0.567	0.566
CCH ₃ ab	0.520	0.520	0.516	0.516
NCH ₃ r	0.768	0.770	0.766	0.768
NCH ₃ ab	0.541	0.531	0.540	0.530
CO ob	0.820	0.810	0.815	0.807
NH ob	0.050	0.043	0.059	0.052
CN t	0.288	0.312	0.304	0.328
CC t	0.008	0.007	0.003	0.002
NC t	0.008	0.013	0.007	0.013

^as=stretch, ss=symmetric stretch, as=antisymmetric stretch, sb=symmetric bend, ab=antisymmetric bend, ib=in-plane bend, ob=out-of-plane bend, d=deformation, r=rock, t=torsion.

^bmdyn Å⁻¹ for stretch and stretch, stretch constants; mdyn for stretch, bend constants; mdyn Å for all others.

so that even if this situation actually exists the refinement would not be changed substantially). We have therefore assigned the major bands to this conformer, using mostly the same general (and non-problematic) assignments arrived at

TABLE 7

Scaled off-diagonal force constants (≥ 0.03) of *trans*-N-methylacetamide

Force constant ^a	Value ^b			
	I	II	III	IV
<i>A'</i> Modes				
1-2	1.221	1.204	1.236	1.214
1-3	0.322	0.319	0.282	0.278
1-4	0.179	0.135	0.183	0.139
1-8	-0.080	-0.059	-0.081	-0.060
1-9	-0.045	0.040	-0.045	0.041
1-10	0.118	0.132	0.121	0.134
1-11	-0.465	-0.404	-0.467	-0.404
1-13	0.186	0.123	0.183	0.118
1-14	0.145	0.137	0.151	0.142
1-16	-0.045	-0.046	-0.044	-0.044
1-20	0.054	0.055	0.055	0.056
1-21	0.029	0.058	0.032	0.057
2-3	0.490	0.485	0.525	0.518
2-4	-0.043	-0.060	-0.043	-0.062
2-6	0.030	0.029	0.026	0.025
2-8	0.031	0.040	0.030	0.041
2-10	-0.470	-0.477	-0.454	-0.460
2-11	-0.077	-0.110	-0.088	-0.120
2-13	-0.004	-0.038	-0.003	-0.039
2-14	0.053	0.056	0.054	0.056
2-16	-0.046	-0.045	-0.047	-0.046
2-17	-0.054	-0.053	0.074	0.072
2-20	-0.058	-0.046	-0.059	-0.047
3-4	-0.025	-0.015	-0.030	-0.019
3-6	0.051	0.053	0.043	0.045
3-10	0.242	0.234	0.267	0.255
3-11	0.268	0.260	0.258	0.249
3-16	-0.225	-0.224	-0.237	-0.235
3-17	0.048	0.048	0.031	0.028
4-8	0.247	0.242	0.244	0.239
4-9	-0.098	-0.081	-0.096	-0.080
4-10	0.041	0.071	0.041	0.071
4-11	0.040	0.090	0.040	0.092
4-13	0.228	0.161	0.232	0.163
4-14	-0.141	-0.157	-0.142	-0.158
4-20	-0.460	-0.462	-0.458	-0.461
4-21	-0.035	-0.046	-0.033	-0.045
5-10	-0.063	-0.061	-0.099	-0.094
5-11	-0.039	-0.045	-0.038	-0.044
5-13	-0.086	-0.072	-0.073	-0.061
6-7	0.097	0.096	-0.020	-0.021
6-16	0.088	0.088	0.097	0.097
7-10	0.087	0.084	-0.108	-0.103

TABLE 7 (Continued)

Force constant ^a	Value ^b			
	I	II	III	IV
7-11	-0.076	-0.075	0.077	0.076
7-17	0.095	0.096	0.080	0.082
7-18	-0.110	-0.110	-0.119	-0.119
8-9	0.138	0.011	0.137	0.010
8-13	-0.039	-0.013	-0.039	-0.013
8-20	0.090	0.098	0.089	0.097
9-10	0.028	-0.007	0.029	-0.008
9-11	0.055	-0.016	0.056	-0.016
9-13	-0.106	0.066	-0.107	0.067
9-21	0.088	0.083	0.089	0.083
9-22	-0.123	-0.138	-0.122	-0.137
10-11	0.171	0.143	0.189	0.160
10-13	0.026	0.087	0.005	0.070
10-16	-0.032	-0.031	-0.060	-0.057
10-17	0.145	0.147	-0.089	-0.095
10-18	0.041	0.038	-0.021	-0.020
11-13	-0.056	0.041	-0.060	0.040
11-14	-0.071	-0.071	-0.070	-0.071
11-17	-0.094	-0.095	0.116	0.115
13-17	0.026	0.025	-0.030	-0.029
13-21	-0.045	0.070	-0.046	0.071
14-21	-0.064	0.039	-0.064	0.038
21-22	-0.037	-0.026	-0.036	-0.025
A'' Modes				
24-26	0.110	0.111	0.112	0.112
24-27	-0.123	-0.123	0.120	0.120
24-30	-0.048	-0.047	-0.046	-0.045
25-28	-0.063	0.064	0.065	0.066
25-29	-0.138	-0.128	0.137	0.127
25-34	-0.025	-0.056	-0.024	-0.056
26-30	-0.120	-0.119	-0.125	-0.125
26-32	-0.021	-0.020	-0.042	-0.041
26-33	-0.051	-0.049	-0.009	-0.009
28-29	0.028	-0.033	0.027	0.032
28-32	-0.036	0.024	-0.039	0.028
28-34	-0.059	-0.064	-0.057	-0.062
30-31	-0.051	-0.036	-0.047	-0.032
30-32	-0.037	-0.057	-0.040	-0.061
30-33	-0.036	-0.034	0.050	0.048
31-32	-0.026	-0.041	-0.036	-0.051

^aNumbers designate symmetry coordinates of Table 4.^bmdyn Å⁻¹ for stretch and stretch, stretch constants; mdyn for stretch, bend constants; mdyn Å for all others.

TABLE 8

Observed and calculated frequencies (in cm^{-1}) of conformers of *trans*-*N*-methylacetamide

Observed			Calculated				PED ^c
$\nu(\text{N}_2)^a$	$\nu(\text{N}_2)^b$	$\nu(\text{A}_\Gamma)^b$	I	II	III	IV	
A' Modes							
3498 s	3495 s	3507 s				3510	
	3490 s	3503 m		3498			NH s(100)
		3500 sh			3496		
			3483				
3008			3047	3028	3048	3002	CCH ₃ as(93) ^d
2973			3029	3001	2993	2992	NCH ₃ as(100) ^d
2958			2918	2931	2929	2932	NCH ₃ ss(100) ^e
2915			2915	2918	2916	2928	CCH ₃ ss(93) ^e
1706 vs	1706 vs	1708 vs	1709	1708	1700	1700	CO s(83) CCN d(11)
1523 m	1524 m	1523 m	1528		1530		
1511 s	1511 s	1509 s					
				1510		1512	NH ib(45) CN s(31)
		1502 m					
1472 vw	1471 vw	1473 vw		1469		1469	
		1459 vw	1460		1459		NCH ₃ ab(82)
1446 w	1445 w	1448 w			1444	1441	CCH ₃ ab(70) CCH ₃ sb(11)
1432 vw	1432 vw	1429 w	1426	1428			CCH ₃ ab(56) NCH ₃ sb(41)
1419 w	1418 w	1417 w		1422		1423	NCH ₃ sb(54) CCH ₃ ab(35)
	1415 vw		1412				NCH ₃ sb(93)
~ 1400 vw	1411 vw	1409 w			1410		
	1369 w	1371 w			1378	1378	CCH ₃ sb(79) CCH ₃ ab(14)
1370 ms							
	1367 m	1365 ms	1375	1375			CCH ₃ sb(87) CC s(11)
1265 ms	1265 ms	1264 ms		1265		1266	NH ib(24) CO ib(20) CN s(15)
							CCH ₃ sb(12)
	1255 sh	1252 ms	1258		1258		
1181 vw				1183		1179	NCH ₃ r(36) NC s(7)
1168 vw			1157		1155		
			1110		1105		
1089 vw				1099		1096	NC s(49) NCH ₃ r(15)
990 vw					985	984	
980 vw			962	961			CCH ₃ r(49) CC s(21)
857 w				859		861	CN s(34) NCH ₃ r(20) CNC d(10)
							CCH ₃ r(10)
			848		851		
658 vw			659	660			CC s(37) CO ib(36)
					649	649	
		442 vw	454		460		
439 w	439 w	437 vw				450	
429 m	429 m	431 m		444			CCN d(50) CO ib(26) CCH ₃ r(17)
		295 vw	302		309		
	279 w	279 w		273		280	CNC d(66) CCN d(34)

TABLE 8 (Continued)

Observed			Calculated				PED ^c
$\nu(\text{N}_2)^a$	$\nu(\text{N}_2)^b$	$\nu(\text{Ar})^b$	I	II	III	IV	
A'' Modes							
3008			2969	2988	2998	2997	NCH ₃ as(100)
2973			2957	2968	2958	2990	CCH ₃ as(101)
	1450 vw	1453 w	1458		1458		NCH ₃ ab(95)
				1441		1441	NCH ₃ ab(85) CCH ₃ ab(10)
1446 w	1445 w	1448 w					
			1440	1440			CCH ₃ ab(83) NCH ₃ ab(10)
1432 vw	1432 vw	1429 w			1429	1429	CCH ₃ ab(92)
			1118	1117	1119	1117	NCH ₃ r(91)
1037 vw			1049	1049	1052	1053	CCH ₃ r(60) CO ob(22)
626 vw					636	639	
619 w			629	631			CO ob(68) CCH ₃ r(33)
			404		409	401	
	439 w	391 s		383			CN t(109) NH ob(43) CO ob(23)
			145	139	155	168	NH ob(84)

^aFrom [14]. ^bFrom [9] and [10]. ^cPotential energy distribution (contributions ≥ 10) for conformer II, unless otherwise noted. ^dReversed for I, III, & IV. ^eReversed for I & III.

by earlier workers [14,24] (small differences will be discussed below). The set of scale factors thus obtained for conformer II was then transferred unchanged to calculate the vibrational frequencies of the other conformers.

Although the force constants for CC torsion (t) and NC t are positive (though small, indicating practically free CH₃ group rotation), off-diagonal constants involving these coordinates are not small and are often negative. As a result, the two lowest calculated frequencies (corresponding to these torsions) were negative. Since this is physically meaningless, we have excluded these two coordinates from the normal mode calculation, which is equivalent to assuming free rotation for both CH₃ groups. While this has no effect on the in-plane frequencies and eigenvectors and a negligible effect on the higher frequency out-of-plane modes, it does influence the lower frequency *A''* modes. We discuss below some specific consequences of this approximation, but we feel that it is probably not possible with the present basis set to obtain a highly accurate description of this part of the potential surface, and therefore some of the quantitative aspects of the low frequency modes must be accepted with caution.

Table 5 presents the scale factors. The scaled force constants are shown in Table 6 (diagonal) and Table 7 (off diagonal ≥ 0.03). In Table 8 we compare the observed matrix-isolated frequencies with calculated values for the four conformers (using the complete force field), giving also the eigenvectors for conformer II (and in some cases for other conformers). We have also computed

the normal modes for all the ND derivatives; these are not tabulated but we will refer to relevant results at appropriate points.

DISCUSSION

Experimental data on matrix-isolated *t*-NMA exist for N₂ [9,10,14] and Ar [9,10] matrices. It is well known that shifts from gas phase frequencies are matrix-dependent, that larger shifts are found in N₂ than in Ar matrices, and that high frequency stretching vibrations give negative shifts while low frequency bending modes show positive shifts [34]. This needs to be kept in mind when comparing band frequencies in the two matrices. Because of the different geometries of substitutional sites in the two matrices, it may also be possible that there are different conformer ratios in these matrices. In one of the studies [14], spectra in a N₂ matrix were compared for deposition from the nozzle at room temperature and at 770 K, significant new bands in the latter being associated with *c*-NMA. Since, as we have seen, the energy difference between *cis* and *trans* NMA is much larger than the differences between conformers of *t*-NMA, it is not only reasonable to expect to see evidence of these conformers in the spectra, but we may also expect to observe changes in associated band intensities with nozzle temperature.

In the NH stretch (s) region, bands are observed at 3507 and 3503 cm⁻¹ in Ar and 3495 and 3490 cm⁻¹ in N₂ [9]. The former pair are close to the gas phase frequency (3501 cm⁻¹ [3]), and the decrease in N₂ can be attributed to the larger interaction shift in this matrix [34]. The presence of two bands was attributed to the co-existence of *c*-NMA and *t*-NMA, but this is unlikely in view of the probable assignment of *c*-NH s to a band at 3458 cm⁻¹ that appears at high nozzle temperature [14]. On the other hand, two NH s bands can be accounted for by the major presence of conformers II and IV, which are expected to have detectably different NH s frequencies (see Table 8). This is due to the difference in NH s force constants (6.775 for II vs. 6.821 for IV), since the bond lengths are the same (Table 2), and reflects the slightly different electronic structures in these different molecular conformations. It might be thought that the band intensities could be used to determine the relative amounts of II and IV in the different matrices, but this would be based on the unwarranted assumption that the relative extinction coefficients are the same for each matrix. It is known that the infrared intensity of the NH s mode is very sensitive to intermolecular interactions [35], and since these might be relatively different for the two conformers in the two matrices, it cannot be assumed that the relative extinction coefficients are unchanged. No bands are obviously assignable to conformers I and III, but a shoulder near 3500 cm⁻¹ in the Ar spectrum might be associated with these structures.

The amide I mode (mainly CO s) has not been examined in sufficient detail to determine if the predicted conformation-dependent splitting is observed.

The amide II mode (mainly NH in-plane bend (ib) plus CN s) is predicted to have a significant dependence on conformation, and the observed bands are completely consistent with this interpretation. In Ar, bands are observed at 1523, 1509, and 1502 cm^{-1} that shift to 1510, 1499, and 1493 cm^{-1} on $^{14}\text{N} \rightarrow ^{15}\text{N}$ substitution [10], isotope shifts of 1.009, 1.007, and 1.006, respectively (bands at 1545 and 1537 cm^{-1} show shifts of 1.001 and 1.003, respectively, and are probably not amide II modes). Comparable bands and shifts are found in N_2 , 1524 (1.010) and 1511 (1.009) cm^{-1} [9], and their shift to $\sim 1480 \text{ cm}^{-1}$ on N-deuteration [14] confirms their assignment to amide II. (The calculated amide II' frequencies are at 1478 (I), 1454 (II), 1481 (III), and 1467 (IV) cm^{-1} , and vary significantly in their CN s component.) The 1523 cm^{-1} band has been assigned to c-NMA [9,10], but this is unlikely: the amide II band of c-NMA appears at 1485 cm^{-1} in the N_2 matrix [14] and near 1495 cm^{-1} in aqueous solution [17,18], and this has been confirmed by ab initio studies [30]. Thus, it is more reasonable to assign the 1523, 1511 cm^{-1} pair to different conformers, and this is well supported by the calculations. These assignments also agree with the observed relative intensities of the bands (conformers II and IV predominating over I and III) and with the relative intensity increase of the higher frequency band for the higher nozzle temperature [14].

The frequencies and eigenvectors in the region of the CH_3 antisymmetric bend (ab) and symmetric bend (sb) modes are very sensitive to the scale factors and conformations. For example, while accepting the assignment of the 1472 cm^{-1} band to a fundamental [14], we find that it is impossible to scale it to an out-of-plane frequency in this region [14] without significantly disrupting the nature of other modes. However, if we assign this band to an in-plane mode, as has been proposed [5], the refinement proceeds satisfactorily, with the appropriate out-of-plane modes being assigned to the 1446 cm^{-1} band. Even within this framework, small changes in scale factors (and therefore force constants) can significantly affect the eigenvectors, so the present descriptions should be considered tentative in detail. Such small intrinsic changes in force constants between conformers (since scale factors are kept the same), undoubtedly combined with the structural changes, therefore account for the significant predicted differences in frequencies and eigenvectors of certain modes. For example, the slightly larger CCH_3 sb force constants for III (0.538) and IV (0.537) than for I (0.530) and II (0.530) could be the main factor determining the slightly higher frequencies of the former two modes; an analogous situation holds for NCH_3 sb. In contrast, the trend in the CCH_3 ab frequencies runs counter to that of the force constants, indicating that structural differences probably play the dominant role in this case.

The observed bands in this region are quite well accounted for by the calculations, including reasonable assignments to conformers. The 1472 cm^{-1} band can be assigned to the NCH_3 ab (A') modes of the predominant II and IV conformers, with the 1459 cm^{-1} band in Ar indicating a larger population

of I and/or III in this matrix. The relative intensity increase in Ar of the 1453 cm^{-1} band, well assigned to the NCH_3 ab (A'') mode, would similarly indicate an enhanced presence of I and/or III in this matrix. The observed bands near 1446 and 1432 cm^{-1} are well assigned to overlapping A' and A'' modes of CCH_3 ab. The enhanced intensity of the 1429 cm^{-1} band in Ar would be consistent with a relatively higher concentration of conformer II in this matrix. The 1418 cm^{-1} band is easily associated with NCH_3 sb (A') of the predominant II and IV conformers, with the weaker 1415 and 1411 cm^{-1} bands being assigned to I and III, respectively. (The latter also show the expected intensity increase with increasing nozzle temperature [14].) If the calculated frequency order is correct, the relative intensity increase of the 1409 cm^{-1} band in Ar would indicate a favored presence of III in this matrix. It is interesting that these modes are predicted to shift on N-deuteration (because of a small NH ib contribution) to 1403 , 1408 , 1402 , and 1404 cm^{-1} for I, II, III, and IV, respectively. The 1418 cm^{-1} band in N_2 does disappear on N-deuteration [10] (the 1419 cm^{-1} band in Ar [10] could be due to a predicted 1419 cm^{-1} CCH_3 ab (A') mode of III, shifted from 1444 cm^{-1}), with the predicted $\sim 1404\text{ cm}^{-1}$ bands possibly appearing as "fine structure" on the dominant HDO band at $\sim 1400\text{ cm}^{-1}$ [10,14]. The CCH_3 sb modes near 1370 cm^{-1} show a splitting [10] consistent with our calculations. The enhanced intensity of the 1365 cm^{-1} band in Ar would again support the previous indications that the concentration of conformer II is relatively higher in this matrix. The predicted effect of N-deuteration, modes of I, II, III, and IV shifting to 1360 , 1356 , 1371 , and 1368 cm^{-1} , respectively, is consistent with observed bands at 1368 and 1360 cm^{-1} [10,14] that are assignable to these modes.

The so-called amide III mode (largely NH ib plus CN s) is also expected to show a conformation dependence, being predicted near 1265 cm^{-1} for conformers II and IV and 1258 cm^{-1} for I and III. Bands are observed at 1265 cm^{-1} in N_2 [9,14] and at 1264 and 1252 cm^{-1} in Ar [10]. These are appropriately assignable to the calculated modes, and are again consistent with a larger proportion of I and/or III in Ar. On N-deuteration, the ND ib mode is predicted at $\sim 904\text{ cm}^{-1}$, and a new band is observed at $\sim 916\text{ cm}^{-1}$ [14].

The NCH_3 rock (r) mode is predicted near 1180 cm^{-1} for conformers II and IV and near 1156 cm^{-1} for I and III. Bands are observed at 1181 and 1168 cm^{-1} [14] that can be satisfactorily assigned to these structures, and that exhibit the expected intensity behavior with increased nozzle temperature [14]. All of these modes are predicted to shift to $\sim 1193\text{ cm}^{-1}$ on N-deuteration, and a new band is indeed found at 1200 cm^{-1} [14]. (The strong band at $\sim 1180\text{ cm}^{-1}$ [14] is undoubtedly due to D_2O .)

The NC s modes for conformers II and IV are well assigned to an observed band at 1089 cm^{-1} . On N-deuteration these modes are predicted to shift to 1137 , 1155 , 1129 , and 1144 cm^{-1} for I, II, II, and IV, respectively, and new bands are observed near 1121 and possibly 1135 cm^{-1} .

While the A'' CCH_3 r frequency is not expected to be conformation dependent, and is assignable to the observed band at 1037 cm^{-1} , the A' modes are significantly sensitive to conformation and would account for observed bands at 990 and 980 cm^{-1} [14]. The nozzle temperature dependence of the relative intensities of these bands [14] would be consistent with conformer I increasing more than III at the higher temperature. On N-deuteration, these bands are predicted to shift to 998 and 977 cm^{-1} , which would be consistent with observed bands at 994 and 979 (sh) cm^{-1} [14].

The mainly CN s mode predicted at $\sim 860\text{ cm}^{-1}$ is observed at 857 cm^{-1} , consistent with its association with the predominant II and IV conformers. Although a conformation sensitivity is indicated, the $\sim 10\text{ cm}^{-1}$ calculated separation is probably in the range of scale factor uncertainty (observed conformer bands are associated with calculated separations of $\sim 25\text{ cm}^{-1}$; compare modes near 1170 and 970 cm^{-1}).

The CN s, CO ib mode near 660 cm^{-1} is well predicted, and again seems not to reflect a predicted conformer splitting of $\sim 10\text{ cm}^{-1}$. However, the CO out-of-plane bend (ob) mode is predicted to show a conformer splitting of only $\sim 8\text{ cm}^{-1}$, yet two assignable bands appear to be present (626 and 619 cm^{-1}). It may be that the absence of the CH_3 t contributions is beginning to be felt for out-of-plane modes in this region.

The CCN deformation (d) mode is predicted to show a splitting of 6 cm^{-1} between conformers IV and II, and we assign the bands observed at 439 and 429 cm^{-1} to these structures, respectively. This assignment requires further discussion, since it has been proposed [9] that the 439 cm^{-1} band in N_2 matrix is an amide V mode (CN t plus NH ob) because its intensity decreases on N-deuteration. It has been suggested [9] that the remaining weaker 439 cm^{-1} band in this case was due to residual undeuterated species, but this is not consistent with a similar result [14] in which the amide II band is essentially absent, indicating that no undeuterated molecules are present. In Ar matrix, weak bands are present at 442 and 437 cm^{-1} [10], the N-deuteration-sensitive amide V mode now being at 391 cm^{-1} . (We discuss below in more detail the assignment of amide V.) Our interpretation, therefore is that CCN d of conformer IV is to be assigned to 439 cm^{-1} , that it is present to a greater extent (compared to II) in the N_2 matrix, and that amide V in N_2 is also at 439 cm^{-1} and overlaps it. It is worth noting that on N-deuteration these bands shift to 436 and 426 cm^{-1} , exactly the 3 cm^{-1} decrease predicted from normal mode calculations.

Skipping amide V for the moment, we see that the CNC d mode is predicted to be conformation-sensitive. The observed bands at 295 and 279 cm^{-1} are assignable to such modes, and their intensities are completely consistent with a preponderance of conformers II and IV and an enhancement in the relative amount of I and/or III in Ar.

The amide V mode presents a special problem, in part because the exclusion

of the CH_3 torsion coordinates from the normal mode calculations makes these predictions more uncertain than those for the high frequency modes. These coordinates have a significant effect, as can be seen from the calculated frequencies of 404, 383, 409, and 401 cm^{-1} in this approximation vs. 447, 339, 449, and 342 cm^{-1} when the torsion coordinates are included, for conformers I, II, III, and IV, respectively. Probably neither calculation is completely accurate. Another aspect of the problem is that two different strong bands are found to be sensitive to N-deuteration, 391 cm^{-1} in Ar matrix [10] and 439 cm^{-1} in N_2 matrix [9]. These have been interpreted in terms of amide V of *t*-NMA and *c*-NMA respectively [9], but we believe that another explanation is more likely. First, we should note that in N_2 there is no 391 cm^{-1} band and in Ar there is no 439 cm^{-1} band (although there are two very weak N-deuteration-sensitive bands at 442 and 437 cm^{-1}). Thus, the above interpretation [9] implies that there is no *t*-NMA in the N_2 matrix, certainly an unsupportable conclusion! Second, the 391 and 439 cm^{-1} bands cannot be correlated with separate conformers, supposedly II and IV (they are too strong for I and III): our analyses of other bands indicated that II and IV are present together (even though the relative amount of II is perhaps larger in Ar), in addition to which the observed separation of 48 cm^{-1} is too large compared with the calculated IV-II difference of 18 cm^{-1} (down to 3 cm^{-1} when CH_3 torsions are included). This 48 cm^{-1} separation, however, would be consistent with the calculated I, III – II difference of ~ 24 (no CH_3 torsions) to 109 cm^{-1} (CH_3 torsions included).

Our interpretation of the amide V modes of *t*-NMA is therefore as follows. In Ar, we assign the 391 cm^{-1} band to conformer II, and probably IV (although a reliable calculated splitting might indicate an assignment of the weak 379 cm^{-1} band to the latter conformer). It is reasonable [34] that the lowest frequency, implying the weakest interactions with the matrix, occurs in Ar. (It is interesting that the lowest amide V frequency obtained in various inert solvents was 418 cm^{-1} in cyclopentane [13].) We assume, following the trend indicated by the torsions-included calculation, that I and III account for the very weak bands at 442 and 437 cm^{-1} . In N_2 , we believe that interactions with the matrix raise the amide V frequency to 439 cm^{-1} , which is a reasonable amount [34]. (In carbon disulfide, the amide V frequency moves up to 470 cm^{-1} [13].) This band is again assigned to II and IV, with I and III associated with the weak N-deuteration-sensitive band at 482 cm^{-1} [9]. The coincidence of the 439 cm^{-1} band with the 442, 437 cm^{-1} bands in Ar is considered fortuitous. While exact details await a more accurate definition of the low-frequency energy surface, we believe that this interpretation is reasonable and is completely consistent with the comparable conclusions reached from the analysis of the rest of the spectrum.

It is important to note, incidentally, that our results provide a possible explanation for the well-known [4,36] but poorly understood [4,37] large breadth of the amide V band in the condensed state: in addition to the obviously large

effect of a range of intermolecular interactions (in this case, a range of hydrogen bond strengths to other NMA (liquid) molecules or to solvent) leading to a range of frequencies, it is clear that conformational isomerism can play a significant role, our normal mode calculations showing a frequency spread of $\sim 25\text{--}100\text{ cm}^{-1}$ between structures in which a $(\text{CH}_3)\text{H}$ atom is *trans* vs. *cis* to $(\text{N})\text{H}$. This may also be the origin of the broad amide V band in the disordered solid phase of *t*-NMA [4].

CONCLUSIONS

Calculations of *ab initio* energies, at either the 4-31G* or 6-31G* levels, show that the energy differences between the four stable conformers of *trans*-NMA are small enough that all four structures would be expected to co-exist at room temperature, and thus to be present in a matrix-isolated sample. Determination of the *ab initio* force fields, scaled to reproduce the experimental frequencies, shows that the conformers should be spectroscopically distinguishable.

We have analyzed the infrared spectra of NMA in Ar [9,10] and N_2 [9,10,14] matrices, and shown that essentially all the observed bands can be interpreted in terms of predicted modes of the expected four conformers. The relative band intensities are consistent with the calculated relative energies of the conformers, as are changes in intensities with temperature.

These results show that it is not necessary to invoke the existence of a non-planar amide group [10] in order to account for the unexpected additional bands in the spectra. The *ab initio* results predict a planar amide group for NMA, as they do for formamide [38] and is confirmed experimentally [39], and our analysis of the NMA spectra is consistent with this conclusion.

The unusually large breadth of the amide V band of NMA in condensed states has not yet had a completely satisfactory explanation. While part of the reason may be the heterogeneity of hydrogen bond interactions, our studies suggest that conformational isomerism may also be a contributing factor. It is clear that such isomerism cannot be neglected in achieving a full understanding of the spectroscopic properties of *trans*-*N*-methylacetamide.

ACKNOWLEDGEMENTS

This research was supported by National Science Foundation grants DMB-8816756 and DMR-8806975.

REFERENCES

- 1 T. Miyazawa, T. Shimanouchi and S. Mizushima, *J. Chem. Phys.*, 24 (1956) 408.
- 2 M. Beer, H.B. Kessler and G.B.B.M. Sutherland, *J. Chem. Phys.*, 29 (1958) 1097.

- 3 R.L. Jones, *J. Mol. Spectrosc.*, 11 (1963) 411.
- 4 E.M. Bradbury and A. Elliott, *Spectrochim. Acta*, 19 (1963) 995.
- 5 B. Schneider, A. Horení, H. Pivcová and J. Honzl, *Collect. Czech. Chem. Commun.*, 30 (1965) 2196.
- 6 K. Itoh and T. Shimanouchi, *Biopolymers*, 5 (1967) 921.
- 7 M. Rey-Lafon, M.T. Forel and C. Garrigou-Lagrange, *Spectrochim. Acta, Part A*, 29 (1973) 471.
- 8 I. Harada, Y. Sugawara, H. Matsuura and T. Shimanouchi, *J. Raman Spectrosc.*, 4 (1975) 91.
- 9 F. Fillaux and C. de Lozé, *J. Chim. Phys.*, 73 (1976) 1004.
- 10 F. Fillaux and C. de Lozé, *J. Chim. Phys.*, 73 (1976) 1010.
- 11 F. Fillaux and C. de Lozé, *Chem. Phys. Lett.*, 39 (1976) 547.
- 12 G. Dellepiane, S. Abbate, P. Bosi and G. Zerbi, *J. Chem. Phys.*, 73 (1980) 1040.
- 13 F. Fillaux and M.H. Baron, *Chem. Phys.*, 62 (1981) 275.
- 14 S. Ataka, H. Takeuchi and M. Tasumi, *J. Mol. Struct.*, 113 (1984) 147.
- 15 L.C. Mayne, L.D. Ziegler and B. Hudson, *J. Phys. Chem.*, 89 (1985) 3395.
- 16 J.M. Dudik, C.R. Johnson and S.A. Asher, *J. Phys. Chem.*, 89 (1985) 3805.
- 17 Y. Wang, R. Purello and T.G. Spiro, *J. Am. Chem. Soc.*, 111 (1989) 8274.
- 18 S. Song, S.A. Asher, S. Krimm and K.D. Shaw, *J. Am. Chem. Soc.*, in press.
- 19 T. Miyazawa, T. Shimanouchi and S. Mizushima, *J. Chem. Phys.*, 29 (1958) 611.
- 20 J. Jakšs and B. Schneider, *Collect. Czech. Chem. Commun.*, 33 (1968) 643.
- 21 J. Jakšs and S. Krimm, *Spectrochim. Acta, Part A*, 27 (1971) 19.
- 22 Y. Sugawara, A.Y. Hirakawa and M. Tsuboi, *J. Mol. Spectrosc.*, 108 (1984) 206.
- 23 T.C. Cheam and S. Krimm, *J. Chem. Phys.*, 82 (1985) 1631.
- 24 Y. Sugawara, A.Y. Hirakawa, M. Tsuboi, S. Kato and K. Morokuma, *J. Mol. Spectrosc.*, 115 (1986) 21.
- 25 A. Balázs, *J. Mol. Struct. (Theochem)*, 153 (1987) 103.
- 26 A. Radzicka, L. Pedersen and R. Wolfenden, *Biochemistry* 27 (1988) 4538.
- 27 W.L. Jorgensen and J. Gao, *J. Am. Chem. Soc.*, 110 (1988) 4212.
- 28 R.H. Barker and G.J. Boudreaux, *Spectrochim. Acta, Part A*, 23 (1967) 727.
- 29 D.C. Rees, M. Lewis, R.B. Honzatko, W.N. Lipscomb and K.D. Hardman, *Proc. Natl. Acad. Sci. U.S.A.*, 78 (1981) 3408.
- 30 N.G. Mirkin and S. Krimm, in J.R. Durig and J.F. Sullivan (Eds.), *XIIth International Conference on Raman Spectroscopy*, Wiley, Chichester, 1990, p. 158.
- 31 M. Kitano, T. Fukuyama and K. Kuchitsu, *Bull. Chem. Soc. Jpn.*, 46 (1973) 384.
- 32 G. Fogarasi and P. Pulay, in J.R. Durig (Ed.), *Vibrational Spectra and Structure*, Elsevier, Amsterdam, Vol. 14, 1985 p. 125.
- 33 E.B. Wilson, Jr., J.C. Decius and P.C. Cross, *Molecular Vibrations*, McGraw Hill, New York, 1955.
- 34 H.E. Hallam (Ed.), *Vibrational Spectroscopy of Trapped Species*, Wiley, London, 1973.
- 35 T. Cheam and S. Krimm, *J. Mol. Struct.*, 146 (1986) 175.
- 36 H.K. Kessler and G.B.B.M. Sutherland, *J. Chem. Phys.*, 21 (1953) 570.
- 37 G. Zerbi and G. Dellepiane, *J. Raman Spectrosc.*, 12 (1982) 165.
- 38 G. Fogarasi, P. Pulay, F. Török and J.E. Boggs, *J. Mol. Struct.*, 57 (1979) 259.
- 39 E. Hirota, R. Sugisaki, C.J. Nielsen and G.O. Sørensen, *J. Mol. Spectrosc.*, 49 (1974) 251.